Ionomer Content Optimization in Nickel-iron-based Anodes with and without Ceria for Anion Exchange Membrane Water Electrolysis

Emily Cossar[a], Alejandro O. Barnett[b,c], Frode Seland[d], Reza Safari[e], Gianluigi A. Botton[e], Elena A. Baranova[a*]

[a] *Department of Chemical and Biological Engineering, Centre for Catalysis Research and Innovation (CCRI) University of Ottawa,161 Louis-Pasteur Ottawa, Canada, K1N 6N5*

[b] *SINTEF Industry, Sustainable Energy Technology Department, New Energy Solutions Group, Trondheim, Norway*

[c] *Department of Energy and Process Engineering, Norwegian University of Science and Technology, NO-7491 Trondheim, Norway*

[d] *Department of Materials Science and Engineering, Norwegian University of Science and Technology, NO-7491 Trondheim, Norway*

[e] *Department of Materials Science Engineering, McMaster University, 1280 Main St. W., Hamilton, Ontario, Canada L8S 4L8*

***Corresponding author email:** elena.baranova@uottawa.ca

***Corresponding author number:** 613-562-5800 ext. 6302

1. Supplementary Information

1.1. Experimental Setup

Figure S1 shows the experimental setup for the AEMWE experiments.

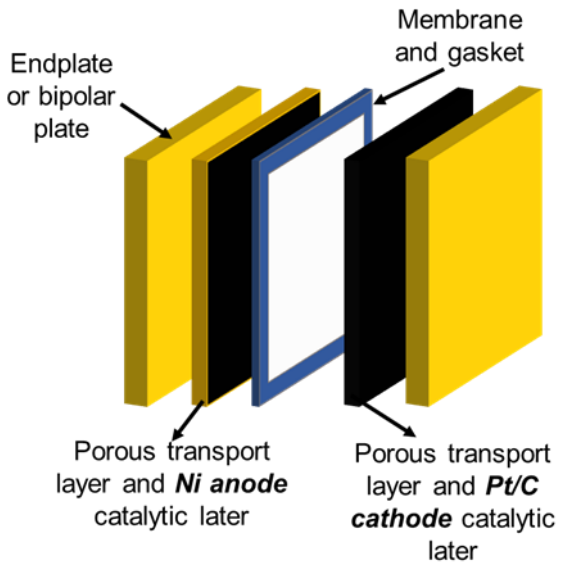

Figure S1: Electrochemical experiment setup for in-situ AEMWE experiments.

1.2. Anode Catalytic Layer Loading

Table S1 shows the actual anode loadings used during every experiment.

Table S1: Anode catalytic layer loadings

Material	**wt% ionomer**	**Desired Loading [mg_{metal} cm^{-2}]**	**Actual Loading [mg_{metal} cm^{-2}]**
Ni	7	5	5.7
Ni	15	5	6.2
Ni	25	5	5.8
$Ni_{90}Fe_{10}$	15	5	5.9
$Ni_{80}Fe_{20}$	15	5	5.4
$Ni_{90}Fe_{10}$ /10 wt% CeO_2	15	5	3.5
$Ni_{80}Fe_{20}$ /10 wt% CeO_2	15	5	3.3
$Ni_{90}Fe_{10}$ *no sonication*	15	5	4.0

1.3. Effect of Ink Preparation on AEMWE Performance

To evaluate the impact of ink sonication on the AEMWE performance, the experiments in Section 2.3.2.2 of the main article were repeated for the $Ni_{90}Fe_{10}$ catalysts, however the amount of sonication used in the ink preparation was reduced. After water and the ionomer was added to the nanoparticles, the sample was sonicated for using 2 mins, then once the IPA was added, the sample was sonicated for 5 mins, both in an ultrasonic bath (45 kHz) over ice. The ultrasonic probe was not used to further sonicate the ink for this experiment. The results of these experiments are presented in Figure S2, with key data presented in Table S2. To see polarization curves without IR-correction, see Figure S3, and to see the best fitted EIS models of the tested electrodes, see Table S3.

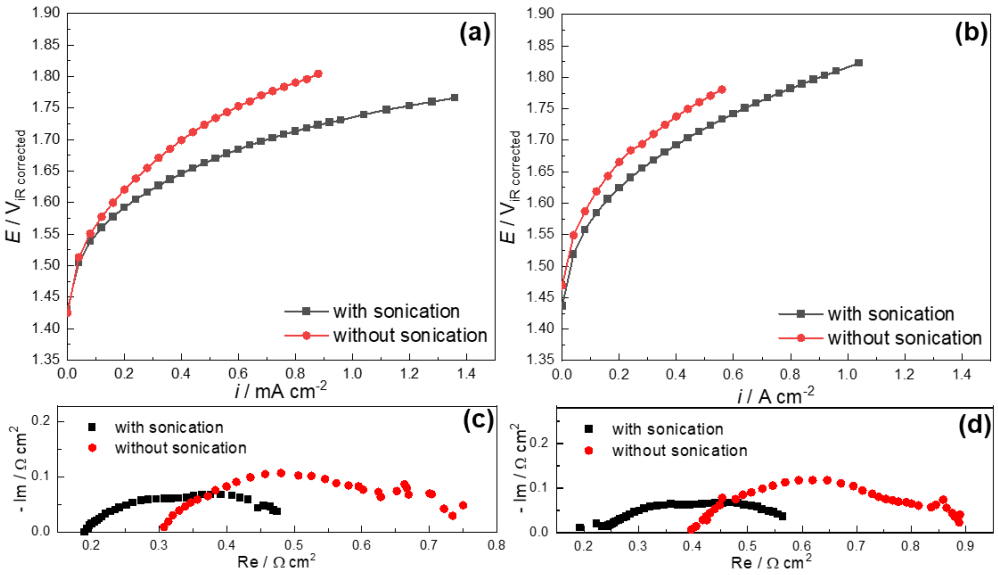

Figure S2: Polarization curves (a, b) and electrochemical impedance spectroscopy run at 5 A (c, d) in 1 (a, c) and 0.1 (b, d) M KOH at 50°C, of the $Ni_{90}Fe_{10}$ catalyst ink with and without sonication.

Table S2: Summary of in-situ sonication performance in 1 and 0.1 M KOH extracted from Figure S2 for the $Ni_{90}Fe_{10}$ ink prepared with and without sonication.

Electrolyte conc. [M]	$Ni_{90}Fe_{10}$ sonication	*E* at 0.4 A cm^{-2} [V]	*E* at 0.8 A cm^{-2} [V]	Tafel Impedance [mV]	R_{EL} [mΩ cm^2]
1	with	1.645	1.717	63	170 ± 3
	without	1.698	1.790	86	286 ± 4
0.1	with	1.692	1.782	70	220 ± 2
	without	1.738	N/A	98	397 ± 3

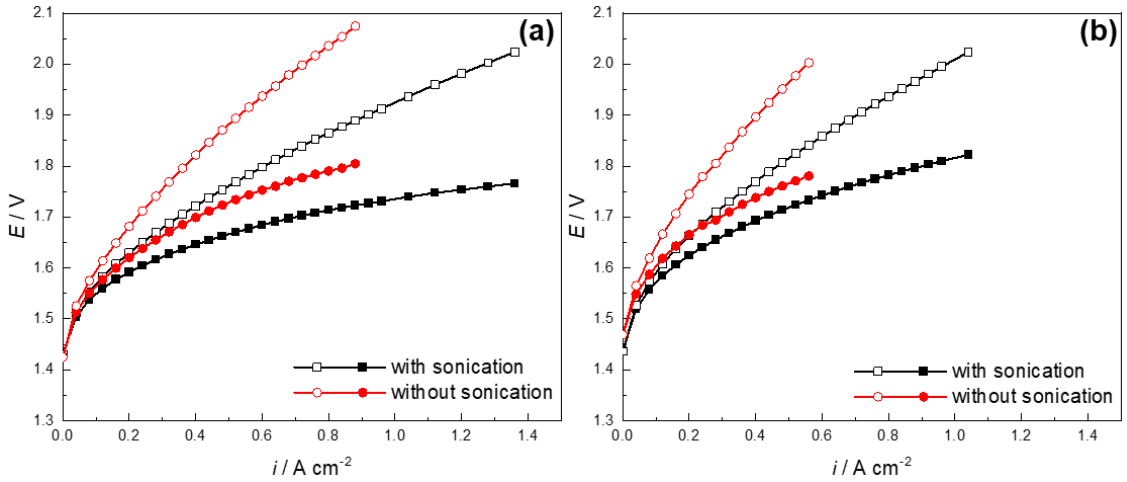

Figure S3: Polarization curves in (a) 1 and (b) 0.1 M KOH at 50°C for $Ni_{90}Fe_{10}$ with and without sonication. The full symbols are the IR-corrected graphs.

As can be seen in Figure S2 and Table S2, sonicating the ink prior to electrode spraying significantly enhances the catalytic activity. However, the electrode loading for the non-sonicated sample was significantly lower (4.0 vs 5.9 mg cm^{-2}) due to lots of waste due to clogging during the spraying. It is therefore possible that the effect of sonication on electrode preparation is mixed with the effect of catalyst loading in the obtained result. As for the polarization and ohmic resistances, they both decreased when the catalyst ink was sonicated. It is possible that this occurs because the lack of sonication resulted in the particles not being properly coated with ionomer and are therefore not well connected to each other within the catalytic layer. Additionally, the low

loading of the non-sonicated sample could decrease the contact between the membrane and the catalyst layer, increasing the ohmic resistance of the system.

1.4. Material Characterization

Figure S4 shows the BJH adsorption pore size distribution measurements by incremental volume (Figure S4a) and area (Figure S4b).

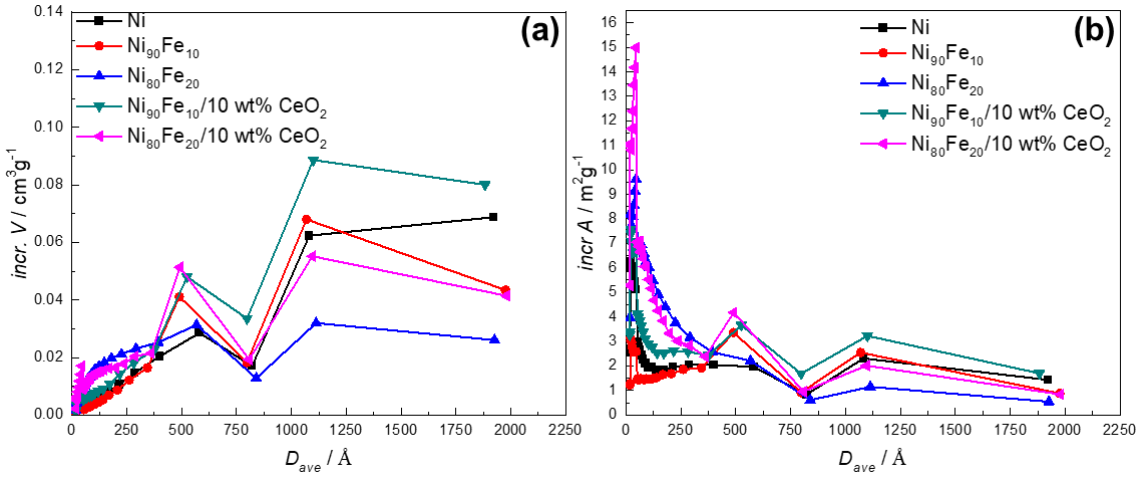

Figure S4: BJH adsorption pore size distribution by incremental (a) volume and (b) area.

1.5. Ionomer Optimization

Figure S5 shows the catalyst coated membranes formed with monometallic Ni nanoparticles and different amount of ionomer, after having been exchanged in KOH for 12 h.

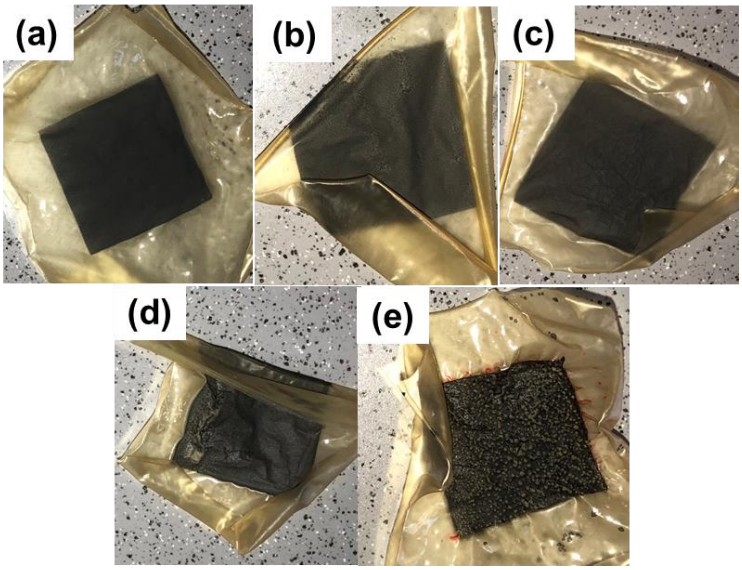

Figure S5: Dried AEMs after ion exchange in 1 M KOH but prior to electrolysis for (a) 7, (b) 15, (c) 25, (d) 35 and (e) 45 wt% ionomer content.

Figure S6 shows how a CCM of Ni NPs with a 5 mg cm^{-2} started to crack and come apart as it was submerged in 1 M KOH.

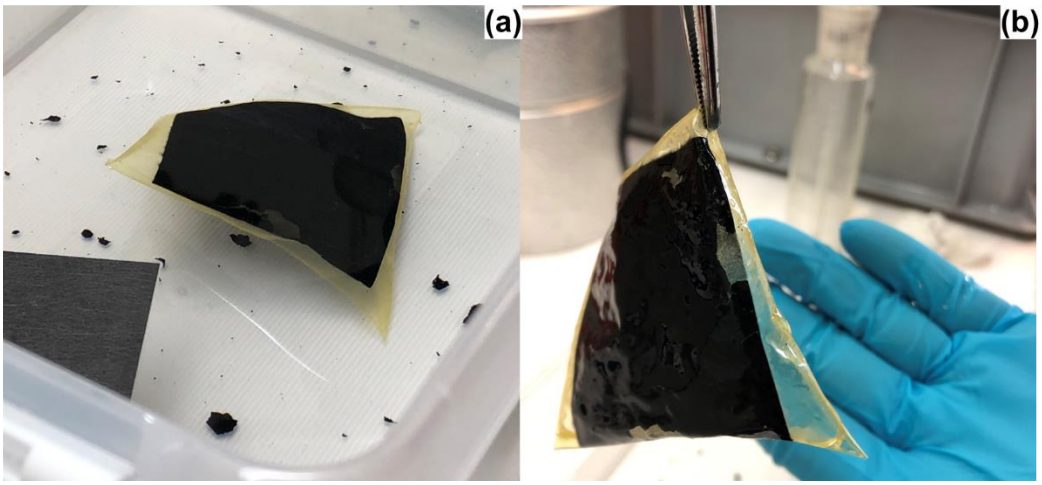

Figure S6: 25 cm^2 CCM (a) exchanging in 1 M KOH (b) removed from KOH when catalytic layer fell off.

Figure S7 shows the polarization curves in 1 M KOH of the ionomer optimization study both with and without IR-correction.

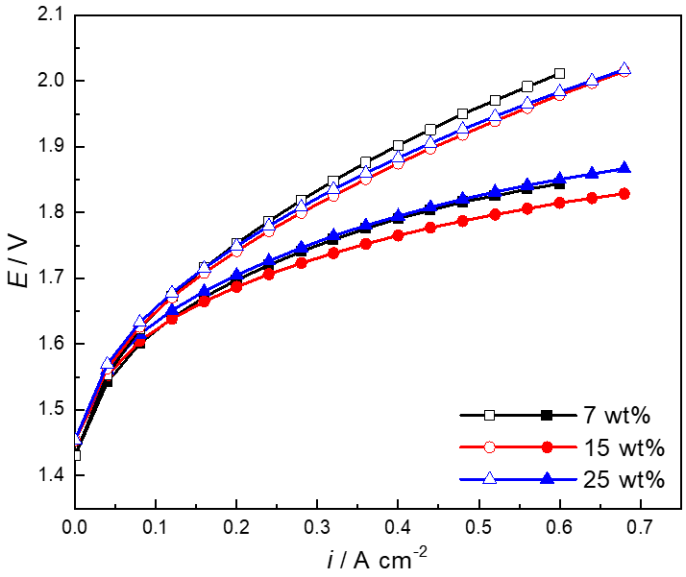

Figure S7: Polarization curves run at 50°C in 1 M KOH for 7, 15, 25 wt% ionomer. The full symbols are the IR-corrected graphs.

Figure S8 shows the polarization curves with and without IR-correction in 1 and 0.1 M for the Ni-based materials tested with the optimized 15 wt% ionomer. Figure S8 also includes the Ir black benchmark electrode.

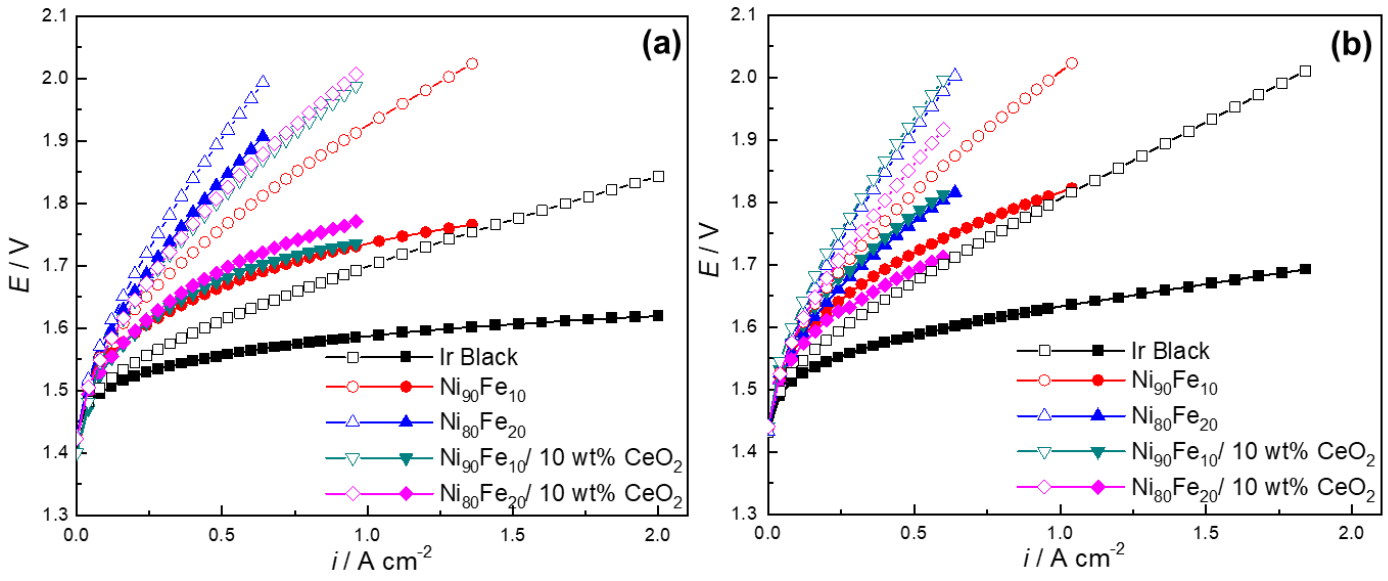

Figure S8: Polarization curves in (a) 1 and (b) 0.1 M KOH run at 50°C. The full symbols are the IR-corrected graphs.

Figure S9 shows the EIS spectra that were obtained every hour over 12 hours during the durability experiments.

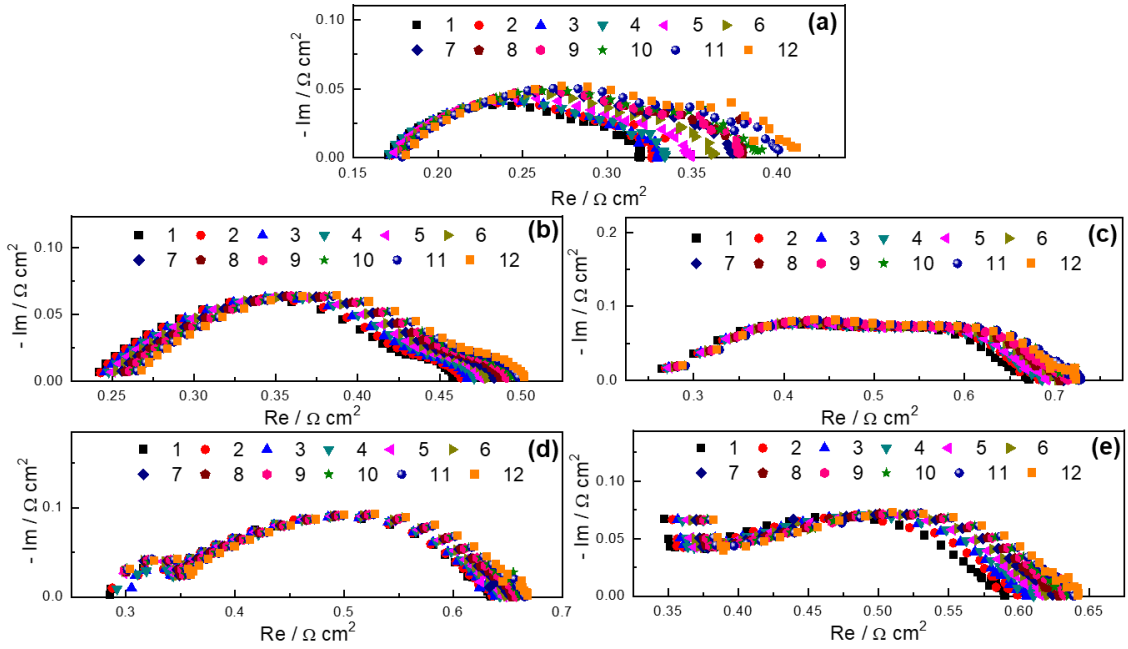

Figure S9: Electrochemical impedance spectroscopy run at 0.5 A cm^{-2} every hour for 12 hours (time indicated in legend) in 0.1 M KOH at 50°C.

1.6. Summary of EIS Fittings

Tables S3 to S7 show the EIS fittings that used to model the experimental data from Figures S2c and d, 4b, 6c and d as well as 8. The data for all EIS spectra was analyzed below 30 kHz, unless otherwise indicated.

Table S3: Summary of EIS models for the plots in Figure S2c and d for $Ni_{90}Fe_{10}$ particles with and without ink sonication in 1 and 0.1 M KOH.

Electrolyte conc. [M]	Material	Circuit Model	L	R_{EL} [mΩ cm^2]	Q_1	n_1	R_1 [mΩ cm^2]	Q_2	n_2	R_2 [mΩ cm^2]
1	$Ni_{90}Fe_{10}$	LR(QR)(QR)	2.44E-04 ± 1.13E-05	170 ± 3	251 ± 59	0.455 ± 0.028	318 ± 64	876 ± 326	1.000 ± 0.405	30 ± 45
	$Ni_{90}Fe_{10}$ no sonication	LR(QR)(QR)	4.88E-04 ± 2.46E-05	286 ± 4	37 ± 7	0.604 ± 0.024	393 ± 21	613 ± 188	1.000 ± 0.158	83 ± 25
0.1	$Ni_{90}Fe_{10}$	R(QR)	---	220 ± 2	250 ± 14	0.415 ± 0.009	406 ± 8	---	---	---
	$Ni_{90}Fe_{10}$ no sonication	R(QR)(QR)	---	397 ± 3	16 ± 2	0.646 ± 0.019	412 ± 17	421 ± 116	0.906 ± 0.119	97 ± 20

Table S4: Summary of EIS models tested for the plots in Figure 4b for Ni NPs with different %ionomer in 1 M KOH.

Material	Circuit Model	L	R_{EL} [mΩ cm^2]	Q_1	n_1	R_1 [mΩ cm^2]	Q_2	n_2	R_2 [mΩ cm^2]
Ni 7 wt%	LR(QR)(QR)	5.33E-04 ± 3.02E-05	254 ± 5	31 ± 6	0.605 ± 0.027	387 ± 19	361 ± 61	1.000 ± 0.084	221 ± 32
Ni 15 wt%	LR(QR)(QR)	7.62E-04 ± 4.45E-05	269 ± 4	848 ± 345	0.737 ± 0.189	354 ± 164	16 ± 6	0.780 ± 0.051	243 ± 29
Ni 25 wt%	LR(QR)(QR)	1.19E-03 ± 3.97E-05	213 ± 3	14 ± 5	0.807 ± 0.048	199 ± 20	589 ± 159	0.778 ± 0.118	338 ± 83

Table S5: Summary of EIS models for the plots in Figure 6c for Ni-based particles in 1 M KOH.

Material	Circuit Model	L	R_{EL} [mΩ cm^2]	Q_1	n_1	R_1 [mΩ cm^2]	Q_2	n_2	R_2 [mΩ cm^2]
Ir Black	LR(QR)(QR)	1.56E-04 ± 1.08E-05	109 ± 1	273 ± 43	0.833 ± 0.070	132 ± 29	184 ± 126	0.722 ± 0.102	46 ± 26
$Ni_{90}Fe_{10}$	LR(QR)(QR)	2.44E-04 ± 1.13E-05	170 ± 3	251 ± 59	0.455 ± 0.028	318 ± 64	876 ± 326	1.000 ± 0.405	30 ± 45
$Ni_{80}Fe_{20}$*	R(QR)	---	130 ± 10	58 ± 5	0.406 ± 0.013	704 ± 18	---	---	---
	LR(QR)(QR)	1.62E-04 ± 3.82E-05	0 ± 54	78 ± 7	0.308 ± 0.030	774 ± 48	14 ± 8	1.000 ± 0.126	77 ± 26
$Ni_{90}Fe_{10}$/ 10 wt% CeO_2	LR(QR)(QR)	8.94E-04 ± 2.26E-05	250 ± 3	34 ± 9	0.683 ± 0.035	242 ± 32	817 ± 221	0.733 ± 0.167	141 ± 49
$Ni_{80}Fe_{20}$/ 10 wt% CeO_2	R(QR)	---	232 ± 6	142 ± 16	0.426 ± 0.018	452 ± 16	---	---	---

*While the LR(QR)(QR) circuit provides a statistically significant better fit, the R(QR) circuit provides an R_{EL} value that is more in line with the value obtained with the raw data. As such, the R_{EL} of the R(QR) circuit is reported in the main text.

Table S6: Summary of EIS models for the plots in Figure 6d for Ni-based particles in 0.1 M KOH.

Material	Circuit Model	L	R_{EL} [mΩ cm^2]	Q_1	n_1	R_1 [mΩ cm^2]	Q_2	n_2	R_2 [mΩ cm^2]
Ir Black	LR(QR)(QR)	1.13E-04 ± 2.39E-05	158 ± 12	247 ± 48	0.790 ± 0.152	144 ± 101	336 ± 617	0.436 ± 0.215	117 ± 127
$Ni_{90}Fe_{10}$	R(QR)	---	220 ± 2	250 ± 14	0.415 ± 0.009	406 ± 8	---	---	---
$Ni_{80}Fe_{20}$	LR(QR)(QR)	2.24E-04 ± 4.10E-05	144 ± 32	117 ± 9	0.296 ± 0.020	695 ± 68	0 ± 0	1.000 ± 0.208	44 ± 35
$Ni_{90}Fe_{10}$/ 10 wt% CeO_2	R(QR)(QR)	---	314 ± 9	448 ± 186	0.320 ± 0.039	438 ± 33	8 ± 3	0.865 ± 0.070	154 ± 35
$Ni_{80}Fe_{20}$/ 10 wt% CeO_2	LR(QR)(QR)	-3.47E-04 ± -2.65E-05	338 ± 5	30 ± 10	0.601 ± 0.045	314 ± 69	1173 ± 616	0.601 ± 0.284	108 ± 86

Table S7: Summary of EIS models for the durability measurement plots in Figure 8 for Ni-based particles in 0.1 M KOH.

Material	Hour	Circuit Model	*L*	R_{EL} [mΩ cm^2]	Q_1	n_1	R_1 [mΩ cm^2]	Q_2	n_2	R_2 [mΩ cm^2]
Ir Black	1*	LR(QR)(QR)	3.42E-04 ± 1.80E-03	101 ± 13544	163 ± 14	0.543 ± 0.025	165 ± 13	1 ± 328	0.672 ± 2.644	58 ± 13543
	12	LR(QR)	3.06E-04 ± 1.60E-05	155 ± 3	190 ± 13	0.455 ± 0.012	256 ± 5	---	---	---
$Ni_{90}Fe_{10}$	1	LR(QR)(QR)	2.23E-04 ± 8.61E-06	202 ± 5	412 ± 77	0.347 ± 0.029	196 ± 6	16 ± 3	0.956 ± 0.041	73 ± 10
	12*	LR(QR)(QR)	1.62E-04 ± 4.30E-03	11 ± 3.99E07	81 ± 9	0.571 ± 0.029	246 ± 18	0 ± 0	0.866 ± 1.19E10	242 ± 3.99E07
$Ni_{80}Fe_{20}$	1	LR(QR)(QR)	2.80E-04 ± 3.68E-05	0 ± 65	21 ± 3	0.362 ± 0.014	621 ± 60	20 ± 6	0.960 ± 0.067	57 ± 10
	12	LR(QR)(QR)	2.79E-04 ± 4.95E-05	10 ± 81	21 ± 4	0.359 ± 0.017	671 ± 76	22 ± 10	1.000 ± 0.101	50 ± 12
$Ni_{90}Fe_{10}$/ 10 wt% CeO_2	1*	R(QR)(QR)	---	3 ± 9067	0 ± 0	1.000 ± 0.708	325 ± 9074	22 ± 1	0.659 ± 0.012	306 ± 6
	12*	R(QR)(QR)	---	10 ± 8037	0 ± 0	0.957 ± 0.684	338 ± 8043	25 ± 2	0.656 ± 0.013	321 ± 7
$Ni_{80}Fe_{20}$/ 10 wt% CeO_2	1	R(QR)(QR)	---	12 ± 744	0 ± 0	0.967 ± 0.232	329 ± 749	34 ± 3	0.623 ± 0.018	249 ± 9
	12**	LR(QR)(QR)	-2.35E-04 ± -4.48E-06	361 ± 3	61 ± 17	0.534 ± 0.032	240 ± 31	23 ± 17	1.000 ± 0.215	44 ± 33

*The circuit fit has a large error, however it was still kept in the table for comparison. ** The data between 50 and 30 kHz of this plot was included to get a better fit.